

## A SHORT-WAVELENGTH MEASUREMENT OF THE COSMIC BACKGROUND RADIATION ANISOTROPY

P. DE BERNARDIS, L. AMICONE, A. DE LUCA, M. DE PETRIS, M. EPIFANI, M. GERVASI, G. GUARINI,  
 S. MASI, AND F. MELCHIORRI

Dipartimento di Fisica, Università La Sapienza, Rome

V. NATALE  
 CAISMI-CNR, Firenze

A. BOSCALERI  
 IROE-CNR, Firenze

AND

G. NATALI, AND F. PEDICHINI  
 IAS-CNR, Frascati

Received 1990 April 3; accepted 1990 June 28

### ABSTRACT

We report the results of a measurement of the CBR anisotropy at wavelengths between 0.4 and 2 mm, carried out using a balloon-borne 1.2 m telescope. We observed a high Galactic latitude region about  $15^\circ$  wide with a  $25'$  FWHM beam, switching in the sky with an amplitude of  $108'$ . A sky signal correlated with the  $100\ \mu\text{m}$  diffuse emission mapped by the *IRAS* satellite was detected and used for calibration. After removal of this contribution, the residual intensity fluctuations give an upper limit to the anisotropy of the CBR at an equivalent frequency of  $9.0\ \text{cm}^{-1}$ . We assumed Gaussian fluctuations with coherence angles between  $5'$  and  $500'$ , and we found upper limits for  $\Delta T/T$  ranging between  $2.2 \times 10^{-4}$  and  $7 \times 10^{-4}$  (95% confidence level).

*Subject headings:* cosmic background radiation — interstellar: grains

### I. INTRODUCTION

Recent measurements of the cosmic background radiation (CBR) spectrum at short wavelengths have shown a close agreement with a thermal spectrum of  $T = 2.735\ \text{K}$  (Mather *et al.* 1990). An excess energy density roughly twice the  $2.7\ \text{K}$  blackbody flux density had been previously reported (Gush 1981; Matsumoto *et al.* 1988). This result strongly supports the standard cosmological model of the hot big bang. However, in this framework, the standard theory of galaxy formation requires perturbations of the primeval fireball and produces anisotropies in the CBR at levels larger than those observed. To solve this problem, the presence of nonbarionic dark matter has been suggested and a large number of theoretical models have been developed. The strong agreement between the CBR spectrum and a pure blackbody excludes the presence of hot gas interacting with CBR photons after the recombination: so small and intermediate-scale anisotropies related to the density perturbations on the last scattering surface are not smeared out and could be measured by sensitive experiments.

Very few anisotropy measurements of the diffuse radiation have been performed at wavenumbers around  $10\ \text{cm}^{-1}$  (Melchiorri *et al.* 1981; Page, Cheng, and Meyer 1990), especially at intermediate angular scales. In this wavelength range lies the maximum of CBR anisotropy flux density. Moreover, the disturbance from radio sources should be a minimum (Franceschini *et al.* 1989).

We describe an anisotropy measurement carried out at wavenumbers between 5 and  $25\ \text{cm}^{-1}$  with an angular scale of  $1:8$ , using a balloon-borne far-infrared telescope (the "ARGO-1989" experiment). In order to maximize the sensitivity to

diffuse radiation, the telescope has been optimized for high throughput and intermediate angular resolution.

### II. INSTRUMENTATION

The instrument was a Cassegrain telescope with a 120 cm diameter,  $f/0.4$  aluminum primary (De Petris, Gervasi, and Liberati 1989) and a wobbling secondary mirror (de Bernardis *et al.* 1989), capable of beam switching with an amplitude of  $1:8$  in the sky. The output optical speed was  $f/3$ . At the focus of the telescope, two detectors were placed. The long-wavelength detector was a composite bolometer cooled to  $0.3\ \text{K}$ , sensitive to radiation in the band  $4.2\text{--}5.5\ \text{cm}^{-1}$  with a large throughput ( $A\Omega = 0.62\ \text{cm}^2\ \text{sr}$ ). This detector had a Winston cone with an input diameter of  $45\ \text{mm}$ : the resulting beam in the sky was  $60'$  FWHM. The short-wavelength detector was a composite bolometer cooled to  $1.5\ \text{K}$ , with a low-pass filter with a slow cut-on at  $\sim 28\ \text{cm}^{-1}$ . Its parabolic cone had an input diameter of  $19\ \text{mm}$ : the resulting beam was  $25'$  FWHM. The beam was split between the two detectors by means of a freestanding wire polarizer. A third detector cooled to  $1.0\ \text{K}$  was not mounted on the gondola due to a liquid helium leak which occurred the night before the flight. The relative spectral efficiency of the detectors is plotted in Figure 1. The telescope was surrounded by a cylindrical superinsulation screen containing eight heat pipes filled with freon; this thermalized the telescope avoiding temperature gradients on the primary mirror. A calibrator consisting of an Eccosorb strip  $4\ \text{cm}$  wide was periodically moved into the beam at a distance of  $280\ \text{cm}$  from the primary mirror, thus providing a calibration signal useful to measure the inflight responsivity and its possible variations. Due to the

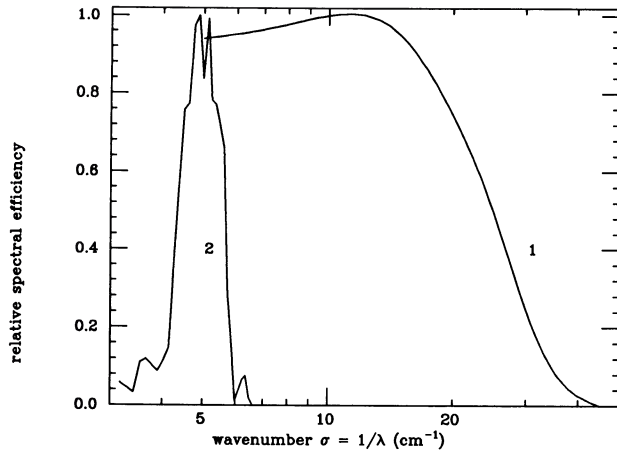


FIG. 1.—Spectral response of the two photometric channels mounted on the experiment. The low-frequency channel (2) was contaminated by RF noise and has not been used for the analysis presented in this Letter.

Rayleigh-Jeans blackbody spectrum of this source and to the wide spectral interval covered in the three detector bands, it was impossible to dimension its emission to calibrate the three detectors simultaneously, so we decided to have an emission high enough to calibrate the two long-wavelength detectors while saturating the high-frequency one.

The telescope was pointed at a fixed elevation angle of  $45^\circ$ ; the azimuth was controlled by an inertial motor system (Boscaleri 1990). The sensor for the azimuth pointing was a three-axis magnetometer with an azimuth sensitivity of about  $1'$ ; the vertical axis was DC amplified with respect to a running offset sampled every 4 minutes; in this way it was possible to detect gondola pendulations at a level of 0.1. A CCD camera (Centurioni, Pedichini, and Natali 1990) was mounted in parallel with the far-infrared telescope, with a field of about  $1.5'$  and a resolution of  $10''$ . The CCD frames were transmitted to ground for real time control of the pointing during the flight. The sensitivity of the CCD was high enough to detect the fainter stars of the SAO catalog with 0.1 s of integration. The instrument was launched from the balloon facility base of Trapani-Milo of the Italian Space Agency at 20:46 UT on 1989 August 9, was flown at a constant altitude of 3.3 mbar, and landed in Spain 23 hr later.

### III. OPERATION DURING THE FLIGHT AND CALIBRATION

Operation of the long-wavelength channel was hampered by RF noise from the telemetry antenna during the flight. We are currently attempting to filter out the spikes produced in the detector signal. Here we report only results from the short wavelength channel which was unaffected by this problem. All the other experiment subsystems worked well during the flight. The modulation amplitude was stable with a maximum long-term variation lower than 0.5% in spite of the large temperature change (from 300 K at ground to about 200 K during the passage through the tropopause). The temperature gradient on the primary mirror did not produce any measurable offset on the high-frequency channel during the night ( $\Delta T < 3 \times 10^{-3}$  K). The calibrator produced a stable signal at constant intervals of 38 minutes, but this cannot be used for absolute calibration of the high-frequency channel due to saturation effects. The CCD camera continuously worked during the night, but at sunrise the background level increased, degrading the image contrast. The pointing system was used to

orient the telescope in several high Galactic latitude regions which were selected for CBR anisotropy measurements. The system is capable of an accuracy of  $6'$  rms during the flight (Boscaleri 1990).

Here we report a preliminary analysis of the data collected around 3:30 UT in the sky strip at declination  $\sim 7^\circ$ ,  $335^\circ < \text{R.A.} < 355^\circ$ . This is a high Galactic latitude region ( $-50^\circ < b < -43^\circ$ ), which is relatively free from large gradients in dust emission, as can be seen from the *IRAS*  $100 \mu\text{m}$  maps: the absolute level of emission is around  $50 \text{ MJy sr}^{-1}$ , while the gradients are lower than  $3 \text{ MJy sr}^{-1}$  at the angular scales of interest here. No point sources are present in this region which could produce a significant signal when diluted in the  $25'$  beam of the high-frequency channel. This sky scan has been obtained by pointing the instrument at a roughly constant azimuth of  $\sim 220^\circ$ , and drift scanning. The raw data have been averaged in 87 independent fields of view ( $25' \times 25'$  pixels) with integration times ranging between 30 and 80 s per field of view. Due to the modulation, each datum represents the measurement of the flux difference between two  $25'$  beams, placed symmetrically with respect to the center of the pixel, at a distance of  $0.9'$  along a modulation direction which forms an angle of  $\sim 45^\circ$  with respect to the scan direction at constant declination. The resulting set of 87 data from the high-frequency channel is plotted in Figure 2, where the data have been divided in four scans at constant declination  $\delta$ . For comparison, the *IRAS*  $100 \mu\text{m}$  data have been convolved with our beam shape and differentiated and are plotted in Figure 2 as a continuous line. A general correlation is evident especially in the scan at  $\delta = 7^\circ 46'$ ; however, significant differences are present in the other scans in the region around  $\text{R.A.} = 340^\circ$ . These are not unexpected, due to the different wavelength bands of the two instruments and to the presence of several

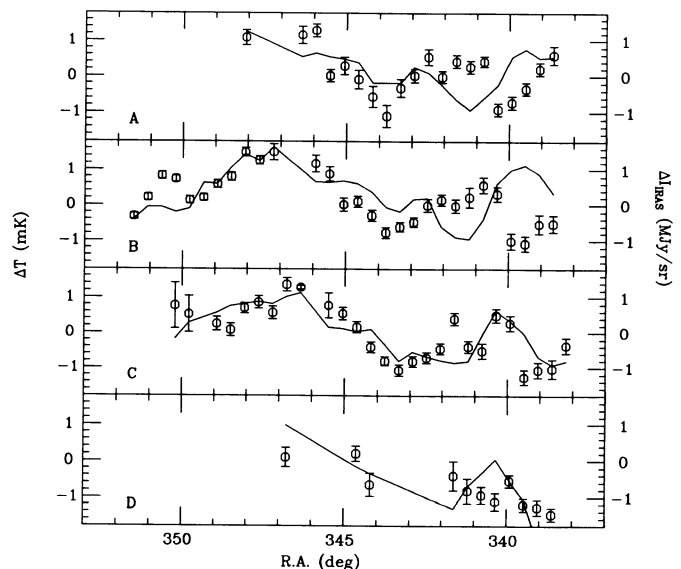


FIG. 2.—Eighty-seven independent single-difference anisotropy data were collected at high Galactic latitudes. They have been divided into four right ascension scans at different declinations (A:  $\delta = 7^\circ 89'$ ; B:  $\delta = 7^\circ 46'$ ; C:  $\delta = 7^\circ 04'$ ; D:  $\delta = 6^\circ 61'$ ) and are plotted vs. the right ascension. The vertical scale is in mK of thermodynamic temperature of the CBR ( $T = 2.75$  K). The continuous line is the signal obtained from the  $100 \mu\text{m}$  survey of the *IRAS* satellite by convolving and differentiating the *IRAS* original data in the same beams observed by our experiment. The vertical units for this signal are  $\text{MJy sr}^{-1}$ .

dust components at different temperatures in the interstellar medium; however, the overall correlation is statistically significant [we have a correlation coefficient of  $(0.57 \pm 0.07)$  with 87 data], and we can conclude that we have detected diffuse dust emission gradients at high Galactic latitudes.

We used this signal to obtain an in-flight calibration of this channel. First of all, we performed a linear best fit between our signals and *IRAS* data. We get the slope  $B$  with a  $2\sigma$  statistical error  $\Delta B/B = 22\%$ . In order to find an estimate of the maximum error on the slope  $B$ , we rebinned the data in 0.4 mK wide intervals, and we built a data subset using the averages over the bins; we used the semidispersion as an estimate of the maximum errors. From the maximum and minimum slope lines, we obtained  $(\Delta B/B)_{\max} = 36\%$ .

To convert this slope in a responsivity measurement, we need to extrapolate the dust spectrum in the wavelength band of our instrument. Obviously this will introduce an additional error in our responsivity estimate. The diffuse dust emission spectrum  $I(\sigma)$  can be extrapolated at longer wavelengths using a dust spectrum which fits the few available observations at high Galactic latitudes: these come from the experiments of Matsumoto *et al.* (1988); Halpern *et al.* (1988); Low *et al.* (1984), and Hauser *et al.* (1984) and are plotted in Figure 3. Only in the *IRAS* survey has the absolute emission at the NGP been observed; when corrected for the zodiacal dust contribution, the emission is  $2.5 \text{ MJy sr}^{-1}$  at  $100 \text{ cm}^{-1}$  (de Bernardis *et al.* 1988). In the other experiments, different regions were observed at high Galactic latitudes and NGP emission has been estimated using a *csc b* law or similar (Halpern *et al.* 1988). A best-fit procedure has been applied to these data using a thermal dust spectrum with temperature  $T_d$  and emissivity  $\epsilon = \epsilon_0 \times \sigma^\delta$ . The best fit parameters are  $\delta_{\text{BF}} = 2.1 \pm 0.8$ ,  $T_{d,\text{BF}} = (20 \pm 4) \text{ K}$ ,  $I_{\text{BF}}(37 \text{ cm}^{-1}) = (5 \pm 3) \times 10^{-14} \text{ W cm}^{-2} \text{ sr}^{-1}/\text{cm}^{-1}$ ; the formal errors are the square roots of the diagonal elements of the covariance matrix. The best-fit curve is also plotted in Figure 3. In order to obtain the in flight responsivity of our instrument, we have computed the expected dust signal

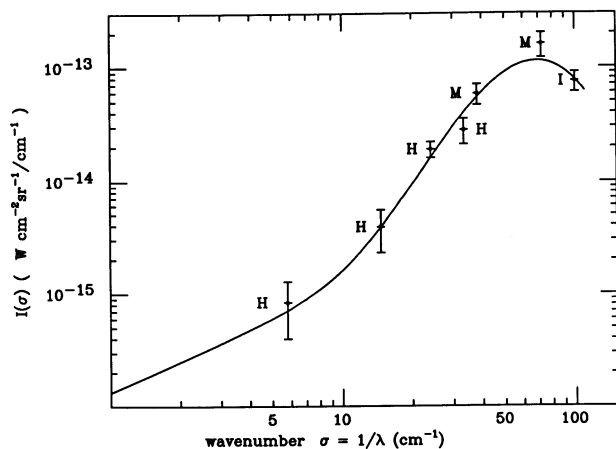


FIG. 3.—Dust spectrum at the north Galactic pole obtained from different observations of diffuse emission. The letters label different experiments: I = *IRAS* survey; H = Halpern *et al.* (1988); M = Matsumoto *et al.* (1988). Only in the *IRAS* survey was the absolute emission at the NGP observed; in the other experiments, other regions were observed at high Galactic latitudes and NGP emission has been estimated using a *csc b* law. The continuous curve represents the best fit to the data I, H, M, using a thermal dust spectrum with temperature  $T_d = 20 \text{ K}$  and a spectral indexes of emissivity  $\delta = 2.1$ . The straight line at long wavelengths is an estimate of the synchrotron contribution (Halpern *et al.* 1988, Fig. 15).

in our detector. This is the convolution  $C$  between our filter band and the dust spectrum  $I(\sigma)$ . We obtained  $C[\delta_{\text{BF}}, T_{d,\text{BF}}, I_{\text{BF}}(37 \text{ cm}^{-1})] = 2.9 \times 10^{-13} \text{ W cm}^{-2} \text{ sr}^{-1}/(\text{MJy}/\text{sr})$ . The error on this quantity was calculated by varying the three parameters  $\delta$ ,  $T_d$ ,  $I(37 \text{ cm}^{-1})$  over a wide range and obtaining the maximum and minimum values of  $C[\delta, T_d, I(37 \text{ cm}^{-1})]$  for which the condition

$$\chi^2[\delta, T_d, I(37 \text{ cm}^{-1})] < [\chi^2(\delta_{\text{BF}}, T_{d,\text{BF}}, I_{\text{BF}}(37 \text{ cm}^{-1})) + \Delta\chi^2] \quad (1)$$

holds. We used  $\Delta\chi^2 = 8.02$  which corresponds to a 95.4% confidence level for the  $\chi^2$  distribution with 3 DOF. We got  $\Delta C/C = 27\%$ . This error is relatively small with respect to the parameters variations because the largest contributions to our signal come from wavenumbers around  $\sim 30 \text{ cm}^{-1}$ , where all the spectra compatible with the condition (1) have very similar intensity. In order to obtain a rough estimate of the maximum error, we repeated the above analysis using  $\Delta\chi^2 = 14.2$  which corresponds to 99.73% confidence level for 3 DOF. In that case we obtain  $(\Delta C/C)_{\max} = 40\%$ .

Statistical errors affecting *IRAS* data are much smaller, but preliminary data from *COBE* question the zero point and gain calibration of *IRAS* data: FIR emission at high Galactic latitudes could be as low as 60% of that measured by *IRAS*. The zero-point error affects calibration only slightly (modifying the dust spectrum around  $100 \text{ cm}^{-1}$  but not the differential signal we used for correlation). On the contrary, if confirmed, a gain error should modify the slope of our correlation, propagating directly to our responsivity calibration: in this case, our upper limits to CBR anisotropy should be reduced accordingly.

We obtain the in-flight responsivity  $R = (5.4 \pm 1.9) \times 10^6 \text{ V/W}$ . The quoted error was obtained by adding quadratically the two sources of uncertainty  $\Delta B/B$  and  $\Delta C/C$  and represents a  $2\sigma$  statistical error. This value of  $R$  is in agreement with the extrapolation of responsivity measurements taken in the laboratory with the same background but at slightly higher temperatures. The maximum error on  $R$  can be obtained by adding linearly  $(\Delta B/B)_{\max}$  and  $(\Delta C/C)_{\max}$ : in that case we obtain  $R = (5 \pm 4) \times 10^6 \text{ V/W}$ .

The best fit of our data with *IRAS* data can be considered a good indicator for the local emission contribution in our wavelength band in the observed region. The residuals from this best fit can be used to search for anisotropies in the extragalactic diffuse radiation at submillimeter wavelengths. The rms value of the residuals (87 independent data) is  $\Delta I = 8.8 \times 10^{-14} \text{ W cm}^{-2} \text{ sr}^{-1}$  in our bandwidth, at the angular scale of  $1'8$ .

#### IV. DISCUSSION

Due to the relatively high frequency of this channel, the measured anisotropy must be compared to several sources of extragalactic radiation. The wide band of the high-frequency channel makes it very sensitive to CBR anisotropies, but also to the diffuse emission due to unresolved extragalactic sources (Franceschini *et al.* 1989), and to fluctuations in any submillimeter extragalactic background.

For the CBR, if we assume a pure blackbody spectrum  $I(\nu, T)$  with  $T = 2.74 \text{ K}$ , we have

$$\frac{\Delta T}{T} = \frac{\Delta I}{\int I(\nu, T)E(\nu)[xe^x/(e^x - 1)]d\nu}, \quad (2)$$

where  $x = h\nu/kT$  and  $E(\nu)$  is the spectral efficiency of the

instrument. The equivalent frequency of our instrument for CBR anisotropies is  $9.0 \text{ cm}^{-1}$ . For our instrument the value of  $\Delta I$  listed above corresponds to an upper limit for CBR temperature anisotropies  $\Delta T/T < 2.4 \times 10^{-4}$  (87 independent fields of view). This rms value gives only a rough estimate of the anisotropy pattern of the CBR. A better analysis can be done by specifying the correlation properties of both the detector noise and the signal to be detected. Using a likelihood ratio analysis, one can take into account the sky coverage, the modulation pattern, and the appearance of the intensity field. Thus, results from different experiments with different characteristics can be compared (Davies *et al.* 1987; Vittorio *et al.* 1989; Redhead *et al.* 1989). Following Davies *et al.* (1987), we assume that the detector noise is uncorrelated in different fields of view, while the intensity fluctuations of the CBR are assumed to have a Gaussian correlation function. The coherence angle  $\theta$  (which defines the average size of the intensity patches) is treated as a free parameter. From our 87 independent data we build up the likelihood ratio  $LR$ , and we change the amplitude  $C_0^{1/2}$  of the intrinsic correlation function in order to search for the maximum of  $LR$ . We will assume that the best value of  $C_0^{1/2}$  consistent with the measured anisotropies is  $C_{0M}^{1/2}$ , corresponding to the maximum  $LR$ , while the formal error on  $C_{0M}^{1/2}$  is calculated finding the values of  $C_0^{1/2}$  for which  $LR = LR_{\text{max}}/10$ : roughly speaking, this corresponds to a confidence level of  $\sim 95\%$ , but the exact statistical distribution can be found only by Monte Carlo simulations. The results are plotted in Figure 4: the level of the upper limit for the intrinsic temperature fluctuations, including both the 95% statistical error in the likelihood analysis and the  $2\sigma$  statistical uncertainty in calibration is  $2\text{--}3 \times 10^{-4}$  for coherence angles between  $15'$  and  $100'$ ; the highest sensitivity is achieved for  $\theta = 45'$ : we have  $C_0^{1/2}/T < 2.2 \times 10^{-4}$ .

Anisotropies are clearly detected, in the sense that the signals are significantly higher than detector noise, and the  $LR_{\text{max}}$  is consequently much larger than 1. However, we must stress the fact that the detected anisotropy can be due to incomplete Galactic dust subtraction, and for this reason it must be considered in any case an upper limit for the extragalactic fluctuations.

If we assume that our upper limit is due to residual dust contamination and if we assume that the dust spectrum is thermal with  $T_d = 20 \text{ K}$  and  $\delta = 2.0$ , we can estimate the level of spurious anisotropy produced by dust at longer wavelengths: we find that in order to have a dust contamination at a

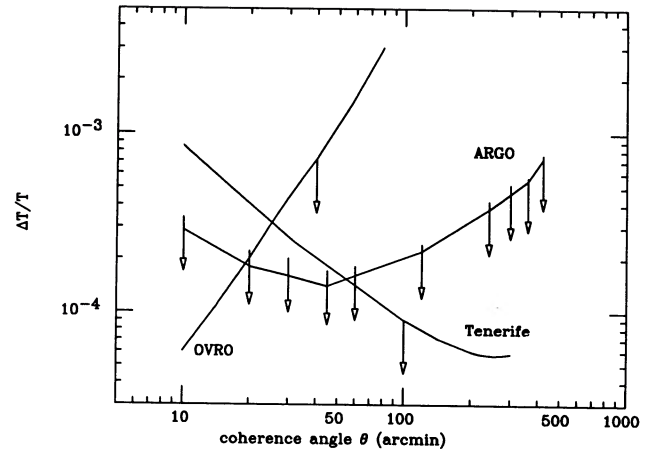


FIG. 4.—Upper limits to the CBR anisotropy in the case of temperature fluctuation pattern described by a Gaussian correlation function with coherence angle  $\theta$ . The intrinsic amplitude of the correlation function  $C_0^{1/2}/T$  is plotted. The detected fluctuations are significantly larger than detector noise but in any case should be considered as upper limits, due to incomplete local emission subtraction. The arrows' upper extremes include both statistical and calibration errors. The other continuous lines shown for comparison are upper limits from the Tenerife experiment (Davies *et al.* 1987) and from the OVRO experiment (Readhead *et al.* 1989).

level  $\Delta T/T \lesssim 1.0 \times 10^{-5}$ , a receiver with central wavenumber  $\sigma_c$  smaller than  $12.5 \text{ cm}^{-1}$  must be used, while for contamination levels lower than  $\Delta T/T \lesssim 1.5 \times 10^{-6}$ ,  $\sigma_c < 5 \text{ cm}^{-1}$ .

Franceschini *et al.* (1989) have estimated the anisotropy resulting from unresolved extragalactic sources: at the equivalent wavenumber ( $\sigma_{\text{eff}} \sim 28 \text{ cm}^{-1}$ ) and in our  $25'$  beam, they expect a minimum anisotropy  $\Delta T/T \sim 1 \times 10^{-4}$  with a source detection limit of  $5\sigma$ : this is still lower than our upper limit.

This work has been supported by Agenzia Spaziale Italiana. We gratefully thank the team of the Base di Lancio di Palloni Stratosferici of ASI in Trapani, especially O. Cosentino, M. Spoto, and A. Leonardi, and the launch team, headed by A. Soubrier of CNES-Toulouse. We thank the Leiden Observatory for the *IRAS* tape (HCON1), used for the correlation between our data and the  $100 \mu\text{m}$  channel. We thank P. Calisse, M. Perciballi, and G. Valmori for their invaluable technical help and D. Mancini of OAC-Napoli for his help in the development of the flight preamplifiers. We also thank the referee for suggestions which improved the error analysis.

#### REFERENCES

- Boscaleri, A. 1990, in preparation.  
 Centurioni, S., Pedichini, F., and Natali, G. 1990, in preparation.  
 Davies, R. D., Watson, R., Daintree, E. J., Hopkins, J., Lasenby, A. N., Beckman, J., Sanchez-Almeida, J., and Rebolo, R. 1987, *Nature*, **326**, 6112.  
 de Bernardis, P., Masi, S., Melchiorri, F., Moreno, G., Vannoni, R., and Aiello, S. 1988, *Ap. J.*, **326**, 941.  
 de Bernardis, P., Masi, S., Perciballi, M., and Romeo, G. 1989, *IR Phys.*, **29**, 1005.  
 De Petris, M., Gervasi, M., and Liberati, F. 1989, *Appl. Optics*, **28**, 1785.  
 Franceschini, A., Toffolatti, L., Danese, L., and De Zotti, G. 1989, *Ap. J.*, **334**, 35.  
 Gush, H. P. 1981, *Phys. Rev. Letters*, **47**, 45.  
 Halpern, M., Benford, R., Meyer, S., Muhelner, D., and Weiss, R. 1988, *Ap. J.*, **332**, 596.  
 Hauser, M. G., *et al.* 1984, *Ap. J. (Letters)*, **278**, L15.  
 Low, F. J., *et al.* 1984, *Ap. J. (Letters)*, **278**, L19.  
 Mather, J. C., *et al.* 1990, *Ap. J. (Letters)*, **354**, L37.  
 Matsumoto, T., Hayakawa, S., Matsuo, H., Murakami, H., Sato, D., Lange, A. E., and Richards, P. L. 1988, *Ap. J.*, **329**, 567.  
 Melchiorri, F., Olivo Melchiorri, B., Ceccarelli, C., and Pietranera, L. 1981, *Ap. J.*, **250**, L1.  
 Page, A. L., Cheng, E. S., and Meyer, S. S. 1990, *Ap. J. (Letters)*, **355**, L1.  
 Readhead, A. C. S., Lawrence, C. R., Myers, S. T., Sargent, W. L. W., Hardbeck, H. E., and Moffet, A. T. 1989, *Ap. J.*, **346**, 566.  
 Vittorio, N., de Bernardis, P., Masi, S., and Scaramella, R. 1989, *Ap. J.*, **341**, 163.

L. AMICONE, P. DE BERNARDIS, A. DE LUCA, M. DE PETRIS, M. EPIFANI, M. GERVASI, G. GUARINI, S. MASI, and F. MELCHIORRI: Dipartimento di Fisica, Università La Sapienza, P.le A. Moro 2, I00185 Rome, Italy

A. BOSCALERI: IROE-CNR, Via Panciatichi, Firenze, Italy

V. NATALE: CAISMI-CNR, Largo E, Fermi, Firenze, Italy

G. NATALI, and F. PEDICHINI: IAS-CNR, Via E. Fermi, Frascati, Italy